NO_x Binding in Hydrated Cementitious Phases

NSF EEC-1757579

Samuel Lucas

Swalm School of Chemical Engineering, Mississippi State University

NNCI Site: SENIC at Georgia Institute of Technology

REU Principal Investigator: Dr. Kimberly Kurtis, School of Civil and Environmental Engineering

REU Mentor: Qingxu (Bill) Jin, School of Civil and Environmental Engineering

Introduction

Nitrogen oxides (NO_x) are a major atmospheric pollutant and contribute to a range of issues, including respiratory ailments, water pollution, acid rain, ground-level smog formation, reduced visibility, and global warming. Despite the implementation of standards, such as EPA emissions standards, NO_x emissions in 2011 exceeded 14 million tons in the U.S. [2]. As such, NO_x presents a major target for further emission reduction. Since nearly 50% of NO_x emissions are due to motor vehicles, strategies targeting emissions along transport routes offer an exciting opportunity for emission reduction [2]. One particularly promising avenue is through the use of cementitious materials, which are omnipresent in infrastructure. Previous research has established that photocatalytic cementitious materials, with the introduction of titanium dioxide (TiO_2), are capable of binding and converting nitrogen oxides (NO_x) to nitrogen ion species (nitrate and nitrite) [4,10,11,12]. Recently, Jin et al [9] has confirmed the NO_x conversion and binding capability in plain ordinary Portland cement (OPC) paste. They have also discovered that the concentration ratio between the conversion products (nitrite:nitrate) is approximately 1:2. This result indicates that there is more nitrate than nitrite formed with plain OPC samples, which could be due to the chemical differences between nitrite and nitrate and their interactions and binding capability with cementitious phases. Therefore, this study examines the interaction of NO_x with individual hydrated cementitious phases to determine the underlying mechanism responsible for NO_x binding.

Two hydrated cementitious phases are examined: the aluminum bearing cement phase AFm (sulfate- and carbonate-substituted), and calcium silicate hydrates (C-S-H). Each of these phases is tested under two conditions: 1) without nitrogen monoxide (NO) exposure and 2) with NO exposure in order to examine the effects of NO exposure in each individual phase. This information allows for the potential optimization of cements for increased NO_x removal and for policy makers to develop new strategies of remediating atmospheric NO_x by taking advantage of the NO_x sequestration capability of existing cement-based infrastructures, such as using them to remediate the NO_x emissions generated in their own production and construction. [6]

Experimental Methods

The aluminum-bearing phase AFm (both sulfate- and carbonate-substituted) was prepared based on the methods proposed by Balonis et al [13]. Calcium silicate hydrates were synthesized in lab from 5 grams of tricalcium silicate (Ca_3SiO_5) and 1.53 grams of silica fume (SiO_2), with 250 ml of deionized water. Reactant amounts were chosen based on previous research on the hydration of tricalcium silicate [15]. The water to solid ratio of 38.3 is selected to ensure a complete reaction and minimize the amount of calcium hydroxide (another product in the reaction) [16]. X-ray diffraction analysis of both AFm and C-S-H confirmed the purity of these substances.

The NO exposure test was designed to follow ISO 22197 and JIS R 1701 [7,8]. 1 gram of sample powder was placed in a borosilicate reactor, which was then exposed under the operating condition. A mix of ultrapure dry air and NO was flowed through the chamber, with the output (as recorded by a Teledyne API Model 200A $NO/NO_2/NO_x$ analyzer) held constant at approximately 1000 ppb. This was performed for a total exposure time of 5 hours.

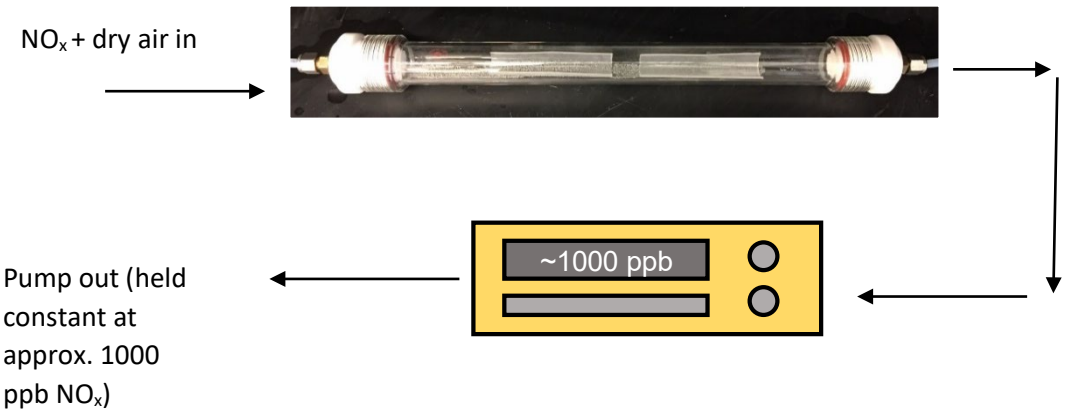

Figure 1. Experimental setup for NO exposure

After exposure, samples were characterized by a number of methods, including x-ray diffraction, Raman spectrometry, and a combination of UV-visible spectrophotometry (UV-vis) and ion chromatography (IC). Raman spectrometry was conducted using a Renishaw Raman Spectrometer with a 785 nm laser at a gradient of 1200. X-ray diffraction (XRD) was conducted using a Malvern Panalytical Empyrean unit equipped with a reflection-transmission spinner stage for powder diffraction, using CuKα radiation and operating at 45 kV and 40 mA. All scans were taken from 5°-80° 2θ.

In order to perform the UV-vis and IC methods, the powder samples were subjected to wet chemical extraction, in which 0.1 gram of sample was mixed with 20 mL of deionized water and shaken for 48 hours. The resulting solutions were filtered through syringe filters and were then stored in a dark environment until analyzed. Nitrite concentration was measured using a colorimetric assay kit (Roche, Sigma-Aldrich) and an Agilent Cary 60 UV-visible spectrophotometer reading at 540 nm. Nitrate concentration was measured using a Dionex ion chromatograph equipped with an Ionpac® AS14A column (4×250 mm) combined with an Ionpac® AG14A guard column (4×50 mm), and a Dionex ED40 electrochemical detector.

Results and Discussion

Unfortunately, Raman spectrometry returned no useable results. Upon examination of unexposed phases (condition 1), it was discovered that all three of the unexposed phases had strong peaks that occurred at the same areas where nitrate and nitrite peaks would have occurred. Examination of exposed samples failed to show any peaks other than those present in non-exposed samples.

The XRD data is illustrated in Figure 2. The XRD spectrum of AFm-SO_4 exposed to NO shows the formation of new peaks that indicate the presence of a nitrate-substituted AFm phase [13]. However, the spectra of the other two NO-exposed phases (AFm-CO_3 and C-S-H) show no distinguishable peaks for nitrogen species, which indicate the unlikelihood of any chemical reactions occurring in these two phases.

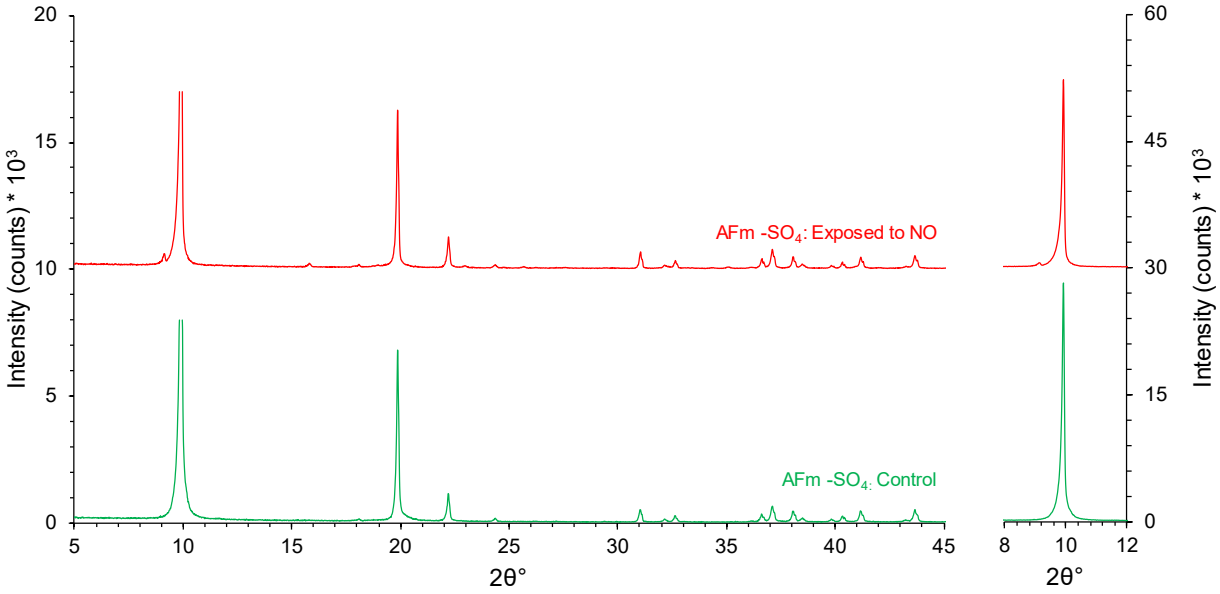
AFm -SO4: Exposed to NO
AFm -SO4: Control
Intensity (counts) * 10^3
2θ°

(a)

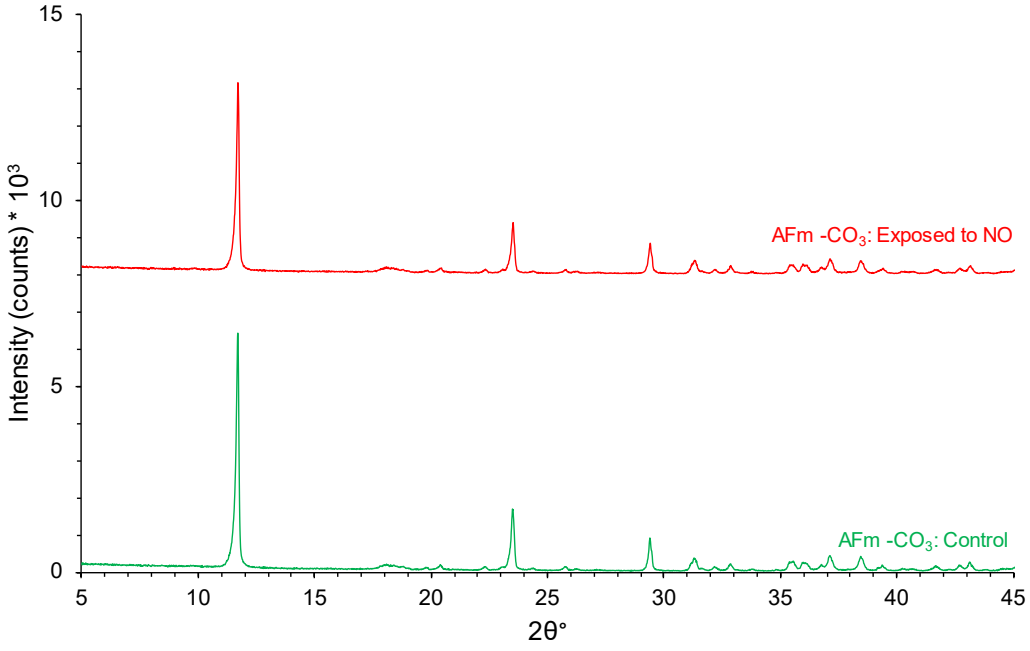
AFm -CO3: Exposed to NO
AFm -CO3: Control
Intensity (counts) * 10^3
2θ°

(b)

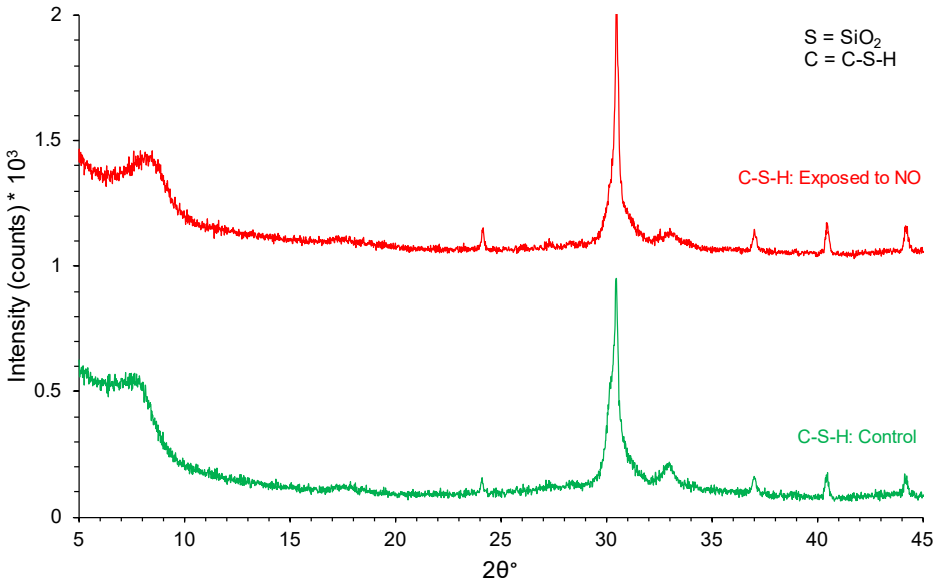

(c)

Figure 1. XRD powder patterns of (a) AFm-SO4 phases, (b) AFm-CO3 phases, and (c) C-S-H phases that are under both NO exposure and control

The UV-vis and IC methods allowed the accurate quantification of nitrite and nitrate concentrations respectively. The R^2 values for the calibration curves were 0.9997 for UV-vis and 0.9836 for IC, indicating a high degree of confidence in the following results.

Group ID	Materials	N mass (mg kg $^{-1}$ hr $^{-1}$)	
		$m_{N\ from\ NO_2^-}$	$m_{N\ from\ NO_3^-}$
1	AFm-SO_4	0.097 ± 0.0004	BDL
2	AFm-CO_3	2.042 ± 0.179	BDL
3	C-S-H	3.997 ± 0.141	1.638 ± 0.488

The relatively high amount of nitrogen ion species formed in plain C-S-H indicates that C-S-H is likely responsible for much of the innate NO_x binding capacity in plain cement. Together with the XRD results, it indicates that the N species are likely physically adsorbed on the surface of the C-S-H phase, which is also the hypothesis proposed by Lee et al [14]. The result of the plain AFm-SO_4 shows a very low amount of N species compared to the other two phases. Again, viewed in conjunction with XRD results, this result indicates a chemical reaction between N species and AFm-SO_4, with the formation of AFm-NO2/NO3, which is believed to be resistant to releasing

nitrite and nitrate in aqueous solution. Future work will incorporate results from NO_2-exposed materials, as well as further characterization of AFm phases to determine whether NO_x binding occurs by chemical substitution rather than physical adsorption, particularly in the AFm-SO_4 phase.

Acknowledgements

I would like to thank the Kurtis group and Dr. Kurtis for hosting me this summer, as well as my mentor Bill Jin for working closely with me and guiding me through the research process. I would also like to thank Leslie O'Neill and Quinn Spadola for all their work throughout the summer. Finally, I would like to thank NNCI and NSF for funding me.

References

1. Jin, Q. (2018). NOx Sequestration by Photocatalytic Concrete. 9th Advances in Cement Based Materials. Pennsylvania State University, 2018.
2. United States, Environmental Protection Agency. (2015). *2011 National Emissions Inventory, Version 2: Technical Support Document.* National Emissions Inventory, U.S. Environmental Protection Agency.
3. J. S. Dalton, P. A. Janes, N. G. Jones, J. A. Nicholson, K. R. Hallam, G. C. Allen, Photocatalytic oxidation of NO_x gases using TiO_2: a surface spectroscopic approach. Environmental Pollution 120 (2002) 415-422.
4. M. M. Ballari, M. Hunger, G. Hüsken, H. J. H. Brouwers, NO_x photocatalytic degradation employing concrete pavement containing titanium dioxide. Applied Catalysis B: Environmental 95 (2010) 245-254.
5. Lee, B. Y., Jayapalan, A. R., Bergin, M. H., & Kurtis, K. E. (2014). Photocatalytic cement exposed to nitrogen oxides: Effect of oxidation and binding. *Cement and Concrete Research,60*, 30-36. doi:10.1016/j.cemconres.2014.03.003
6. Al-Mehthel, M., Al-Dulaijan, S., Al-Idi, S. H., Shameem, M., Ali, M., & Maslehuddin, M. (2009). Performance of generic and proprietary corrosion inhibitors in chloride-contaminated silica fume cement concrete. *Construction and Building Materials, 23*(5), 1768-1774. doi:10.1016/j.conbuildmat.2008.10.010
7. International Organization for Standardization. (2016). *Fine ceramics (advanced ceramics, advanced technical ceramics) — Test method for air-purification performance of semiconducting photocatalytic materials — Part 1: Removal of nitric oxide.* (ISO Standard No. 22197). Retrieved from https://www.iso.org/obp/ui/#iso:std:iso:22197:-1:ed-2:v1:en

8. Japanese Industrial Standard. (2016). *Fine ceramics (advanced ceramics, advanced technical ceramics) -- Test method for air purification performance of photocatalytic materials -- Part 1: Removal of nitric oxide (Foreign Standard)*. (JIS R 1701). Retrieved from https://standards.globalspec.com/std/10063458/jsa-jis-r-1701-1

9. Jin, Q., Saad, E., Zhang, W., Tang, Y., & Kurtis, K.E. (2018). Quantification of Nitric Oxide Binding in Plain and TiO_2-doped Cementitious Materials. Manuscript submitted for publication.

10. Ballari, M.M., Yu, Q.L., Brouwers, H.J.H. Experimental study of the NO and NO_2 degradation by photocatalytically active concrete. Catalysis Today 161 (2011) 175-180.

11. Dylla, H., Hassan, M.M., Schmitt, M., Rupnow, T., Mohammad, L.N. Laboratory Investigation of the Effect of Mixed Nitrogen Dioxide and Nitrogen Oxide Gases on Titanium Dioxide Photocatalytic Efficiency in Concrete Pavements. Journal of Materials in Civil Engineering 23 (2011) 1087-1093.

12. Jayapalan, A.R., Lee, B.Y., Land, E.M., Bergin, M.H., Kurtis, K.E. Photocatalytic Efficiency of Cement-Based Materials: Demonstration of Proposed Test Method. ACI Materials Journal 112 Issue 2 (2015) 219-228.

13. Balonis, M., Medala, M., & Glasser, F. P. (2011). Influence of calcium nitrate and nitrite on the constitution of AFm and AFt cement hydrates. Advances in Cement research, 23(3), 129-143

14. Lee, B. Y., Jayapalan, A. R., Bergin, M. H., & Kurtis, K. E. (2014). Photocatalytic cement exposed to nitrogen oxides: effect of oxidation and binding. Cement and Concrete Research, 60, 30-36

15. Allen, A.J., Thomas, J.J., & Jennings, H.M. (2007). Composition and density of nanoscale calcium-silicate-hydrate in cement. Nature Materials, 6, 311-316.

16. Bernard, E., Lothenbach, B., Le Goff, F., Pochard, I., & Dauzères, A. (2017). Effect of magnesium on calcium silicate hydrate (C-S-H), Cement and Concrete Research, 97, 61-72.